

An Appropriate Specimen Configuration for Evaluating the Perforation Corrosion Resistance of Automotive Coated Steel Sheets in Accelerated Corrosion Tests

Daisuke Mizuno,^{†*} Katsuya Hoshino,^{*} Shinji Otsuka,^{*} Sakae Fujita,^{**} and Nobuyoshi Hara^{***}

ABSTRACT

A variety of metallic coatings have been developed for automotive steel sheet panels to achieve better corrosion resistance. Accelerated corrosion tests are used to develop and select coated steel sheets in a short period. In addition to the test conditions, a specimen configuration simulating the lapped portion of vehicles is another important issue when evaluating resistance to perforation corrosion in the laboratory since the specimen must reproduce the unique environment inside the lapped portion. In this study, lapped specimens with different configurations were prepared and the influence of a bare area in a large crevice on the corrosion behavior of zinc coatings was systematically analyzed by comparing the results of laboratory tests with the corrosion observed in vehicles in service. It was found that the controlling factor of resistance to perforation corrosion was influenced by the configuration of the test specimen. A large crevice gap and bare area in the crevice of the lapped portion changed the corrosion behavior of the coatings and solution within the crevice. As a result of this, the corrosion of pure zinc was accelerated in comparison with zinc alloy coatings due to the rapid corrosion rate of the coating and the rapid consumption of corrosion product in the crevice. On the basis of the experimental findings, an appropriate specimen configuration and specimen preparation procedure for evaluating perforation corrosion resistance were proposed.

KEY WORDS: automobile, coated steel, corrosion test, perforation, specimen, zinc

INTRODUCTION

A variety of metallic coatings have been developed since the 1970s to prevent the corrosion of steel sheets for automobiles in response to corrosion problems caused by the deicing salt that was spread on the road in winter in the United States.¹⁻⁴ Soon after this problem was identified, the salt spray test (SST) was used to evaluate the corrosion resistance of coatings to shorten the testing period. Since it was recognized that the correlation between the corrosion behavior in the SST and that in actual-use environments was poor, automakers and steel makers have developed many types of cyclic corrosion tests (CCT).⁵⁻⁸ However, their reliability for predicting the corrosion resistance of zinc and zinc alloy coatings under in-service conditions has not been fully confirmed.

The typical corrosion morphologies observed in automobiles are cosmetic corrosion and perforation corrosion. The Society of Automotive Engineers (SAE, Warrendale, Pennsylvania) has developed a cosmetic corrosion testing method based on the correlation between on-vehicle tests and standardized methods, such as SAE J2334.⁹⁻¹³ Painted panels with artificial defects are used in corrosion tests to evaluate cosmetic corrosion resistance. These tests are commonly used for developing not only metallic coatings but also chemical conversion treatments and paint systems. On the other hand, in spite of the fact that

Submitted for publication: March 30, 2014. Revised and accepted: September 9, 2014. Preprint available online: September 16, 2014. doi: <http://dx.doi.org/10.5006/1298>.

[†] Corresponding author. E-mail: d-mizuno@jfe-steel.co.jp.

^{*} JFE Steel Corp., Steel Research Laboratory, 1 Kokan-Cho Fukuyama, Hiroshima 721-8510, Japan.

^{**} JFE Techno Research Corp., 1 Kokan-Cho Fukuyama, Hiroshima 721-0931, Japan.

^{***} Tohoku University, Department of Materials Science, Graduate School of Engineering, Tohoku University, 6-6-02 Aobayama, Aoba-ku, Sendai 980-8579, Japan.

perforation corrosion is one of the major corrosion issues requiring a solution in the automotive industry, an accelerated corrosion test with a good correlation with the perforation corrosion observed in vehicles in service has not yet been established. The authors of this study have proposed a method for evaluating the correlation of perforation corrosion in corrosion tests and vehicles in service.¹⁴ For evaluation of perforation corrosion resistance from corrosion tests, many types of configurations of the test specimens have been developed to simulate the lapped portions where perforation corrosion occurs in vehicles.¹⁵⁻¹⁹ In some cases, the lapped specimen was assembled using painted materials with an intentionally bare metal area. In addition, spacers were installed between two panels to adjust the crevice gap of the lapped specimen to prevent corrosion data from having variation. Davidson, et al., reported that a 250 μm -thick spacer was used to obtain a constant clearance in lapped specimens and this spacer was applied to establish an evaluation method for perforation corrosion using SAE J2334 test conditions.¹³ A lapped specimen with a crevice gap of 120 μm is widely used in Europe.¹⁹ However, the influence of the bare area and the crevice gap in the lapped specimen on the perforation corrosion behavior of coated steel is still not well understood. Use of an inadequate specimen that does not reproduce the corrosion mechanism in actual-use environments can be misleading in the development and selection of corrosion-resistant materials. In this study, to identify an appropriate test specimen configuration for evaluating perforation corrosion resistance, the influence of the specimen's configuration on the corrosion behavior of zinc-coated steels was investigated using an accelerated corrosion test, and the test results were compared with the corrosion behavior of a vehicle in service.

EXPERIMENTAL PROCEDURES

Materials

The materials used in this study are shown in Table 1. The sample materials were carbon steel (cold-rolled mild steel, CR), pure zinc-coated, and zinc alloy-coated steel sheets manufactured for automotive body panels. Electroplated steel (EG) and hot-dip galvanized steel (GI) had pure zinc coatings (purity >99.9 wt% for EG and >99.0 wt% for GI). The zinc-nickel electroplated coating (ZnNi) was deposited by electroplating and contained 12 wt% to 13 wt% Ni. The galvanized coating (GA) was an iron-zinc alloy coating formed by continuous heat treatment after the hot-dip galvanizing process. The thickness of the steel sheets was 0.7 mm to 0.8 mm, which is the ordinary range for automotive outer panels. Both sides of the steel sheets were coated and the coating weight for each side was 20 g/m^2 to 100 g/m^2 . The substrate steels of all the coatings was mild steel.

TABLE 1
Materials

Material/Coating	Symbol	Coating Weight (g/m^2)	Remarks
Carbon steel (mild steel)	CR	0	
Electroplated steel	EG	20, 50	
ZnNi electroplated steel	ZnNi	35	Ni 12.8 wt%
Galvanized steel	GA	40	Fe 10.7 wt%
Hot-dip galvanized steel	GI	50, 65, 100	

Sample Preparation

Lapped specimens were prepared to analyze the perforation corrosion behavior of coated steel sheets. A schematic drawing of a specimen is shown in Figure 1. Specimens were assembled by spot welding two pieces of the same material. The welding pressure was 2.5 kN and the welding current was optimized so that the diameter of the weld nugget was larger than $4\sqrt{t}$ (where t is the thickness of steel) without sputtering. The influence of the bare area, which was intentionally formed inside the crevice, and the crevice gap on corrosion behavior were investigated using specimens of the same shape. For investigating the influence of the crevice gap and bare area in the crevice, specimens with two configurations were prepared, as shown in Figure 2. In Configuration A, two pieces of the same material were placed in direct contact with each other and welded. After the spot welding, alkaline degreasing, surface conditioning, phosphating, and electrodeposition were performed and specimens were baked at 170°C to form paint. The solution for phosphating was a zinc phosphating type and the paint was an epoxy system for cathodic deposition, which were applied for the commercial mass production of automobiles. The thickness of the electrodeposited paint after baking was adjusted by controlling the voltage and was approximately 20 μm thick on the outer surface of the specimen. In this case, a bare area formed naturally inside the lapped portion because of the small crevice gap (<50 μm).

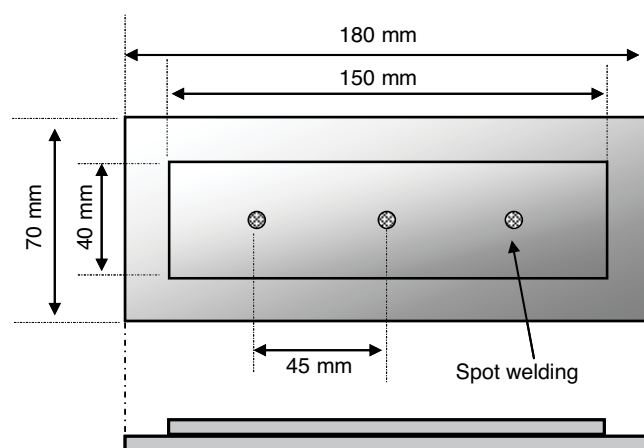


FIGURE 1. Configuration of lapped specimen for corrosion test.

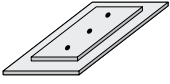
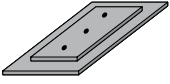
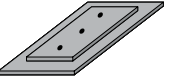
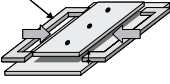
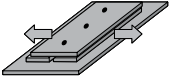
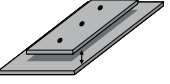
Configuration	Sample Preparation		
	(1) Assembly (spot welding)	(2) Phosphating and painting	(3) Final shape
Configuration A Without adjusting the clearance	 Two on top of each other directly		 Clearance <math>< 50 \mu\text{m}</math>
Configuration B Clearance of 300 μm bare area in the crevice	 Insert spacers The clearance was adjusted by the plastic spacers	 Remove spacers Spacer was removed after paint deposition (before baking)	 Bare area is formed in the crevice with wide clearance

FIGURE 2. Preparation of lapped specimen for corrosion test.

On the other hand, in Configuration B, a bare area and large crevice gap were intentionally created by using 300 μm -thick plastic spacers. Although the specimen had a crevice gap, weld nuggets were formed at the center due to the welding pressure of 2.5 kN. A bare area was formed in this large crevice by performing phosphating and electrodeposition with spacers inserted in the crevice. The specimens with Configuration B had the same shape as Configuration A with a bare area in the larger crevice. To investigate the influence of the crevice gap on corrosion behavior, configuration B specimens with different crevice gaps (100, 200, and 300 μm) were also prepared using GI 100 g/m^2 . The crevice gap was adjusted by the thickness of the plastic spacer. The corrosion rate and the amount of zinc corrosion product in the crevice with different gaps were compared. The specimens were baked after the spacers were removed. In addition, the specimens in which electrodeposition was applied without the spacer were prepared to compare the throwing power, which is defined by how far paint can penetrate in to the crevice from the gap mouth. It is noted that the average crevice gaps were 74, 194, and 279 μm when using spacers with thicknesses of 100, 200, and 300 μm , respectively. For convenience, the crevice gap is represented by the spacer thickness in this paper.

Corrosion Testing and Evaluations

A CCT was carried out and the corrosion damage on the specimens was quantitatively evaluated. Since there is no perforation corrosion test method that displays good correlation with the corrosion of vehicles in service, SAE J2334 was used in this study, since this method is regarded as the most reliable method for evaluating cosmetic corrosion.⁹⁻¹³ The details of the SAE J2334 corrosion test conditions are shown in Figure 3.⁹ Salt was applied by dipping the speci-

mens in the specified 0.5% sodium chloride (NaCl) + 0.1% calcium chloride (CaCl₂) + 0.075% sodium hydrogencarbonate (NaHCO₃) solution. Specimens were placed in the corrosion chamber so that the surfaces of the specimens were at approximately 60° to the horizontal. The corrosion test was not replicated in this study, although multiple sets of specimens were evaluated.

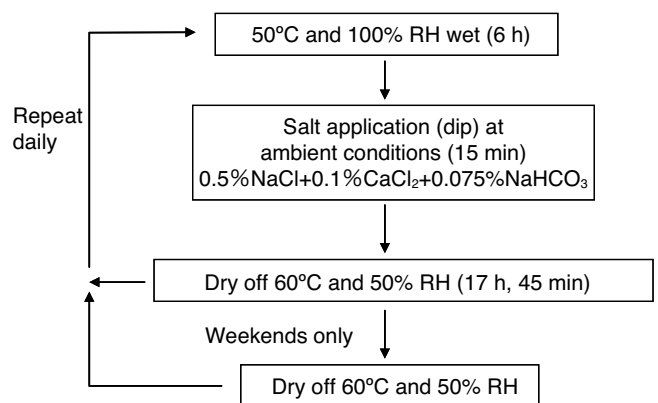


FIGURE 3. Test condition of SAE J2334—manual operation.

Specimens were taken out from the corrosion chamber after 60 cycles. The lapped specimens were then disassembled by removing the weld nuggets with a drill. After observation of the corroded inner surface in the crevice, the paint was removed with a paint remover (NEOS[†] CS500) and the corrosion product was chemically and mechanically removed by brushing with a wire brush in an 18 wt% hydrochloric acid (HCl) + 3.5 g/L hexamethylenetetramine ([CH₂]₆N₄) solution in accordance with the ISO 8407 C.3.5 method.²⁰

To quantify perforation corrosion, the corroded area, after the corrosion product was removed, was divided into 10 unit areas (15 mm by 20 mm) for each

[†] Trade name.

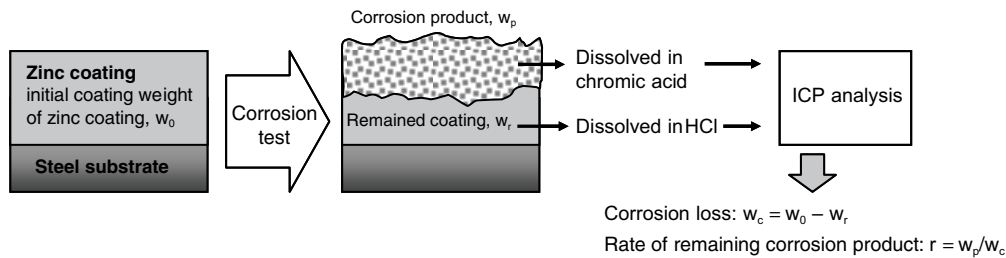


FIGURE 4. Determination of corrosion loss and the amount of remaining corrosion product by ICP analysis.

piece by drawing grid lines, and the minimum thickness of the steel in each unit area was measured with a point micrometer. The maximum corrosion depths in the unit areas were determined from the difference between the initial thickness and the minimum measured thickness after the test. The mode of the maximum corrosion depth was estimated from a Gumbel distribution by using the data of the maximum depth measured in 20 units gritted on both sides of the lapped specimen.²¹⁻²²

The amount of corrosion and the corrosion product of the coating were quantified by introduced coupling plasma (ICP) analysis. Analysis was conducted for one of two specimens. The zinc corrosion product deposited on an area of 30 mm by 100 mm inside the crevice was chemically dissolved by immersion in chromic acid (H_2CrO_4) at 80°C, as specified in ISO 8407 C9.3.²⁰ The remaining zinc coating after removing the corrosion product was then dissolved in 12 wt% HCl. Those solutions were analyzed by ICP and the amounts of the corrosion product and remaining coating were determined as the amounts of zinc from Equation (1):

$$[Zn] = C_{Zn} \times r \times V/S \quad (1)$$

where [Zn] is the amount of corrosion product or remaining zinc coating (g/m^2), C_{Zn} is the concentration of zinc from the ICP measurement (g/L), r is the dilution ratio, V is the volume of solution (L), and S is the area (m^2) in which the corrosion product and remained coating were dissolved.

Consumption of the coating as a result of corrosion was also quantified from the difference between the initial and remaining coating weight. A schematic illustration of the procedure for calculating the consumption of the coating and the amount of corrosion product is shown in Figure 4.

Polarization Curve Measurement

Potentiodynamic curves of the coated steel sheets (GI, GA, and ZnNi) were measured to investigate their corrosion behavior under different conditions. Measurements were conducted in a 5 wt% NaCl solution in air and with deaeration using nitrogen gas. A three-electrode system using a platinum counter electrode and silver/silver chloride ($Ag/AgCl$) in saturated po-

tassium chloride (KCl) as a reference electrode was used. After measuring the corrosion potential for 10 min, the anodic curve and cathodic curve were separately measured. The potential was swept from the open-circuit potential (OCP) to $-0.6 V_{Ag/AgCl}$ for the anodic curve and from the OCP to $-1.7 V_{Ag/AgCl}$ for the cathodic curve at 20 mV/min. The measurement in each condition was replicated twice.

RESULTS

Results of Perforation Corrosion Testing

The appearances of specimens disassembled after a 60-cycle corrosion test are shown in Figure 5. With carbon steel, ZnNi, and GA, the surfaces of the configuration A specimens were covered with red rust from iron. Most of the surface of the GI was covered with white rust from zinc, and the red rust attributed to the corrosion of the steel substrate was slight. A thick coating of $100 g/m^2$ seemed to prevent corrosion effectively. In the case of configuration B, remarkable corrosion damage was not seen in ZnNi and corrosion of the coating itself even seemed to be slight. In contrast to this, the damage of the other coatings was severe and the specimens were covered with red rust. Therefore, it was found that the corrosion test results strongly depend on the configuration of the test specimen, even when the test conditions are completely identical.

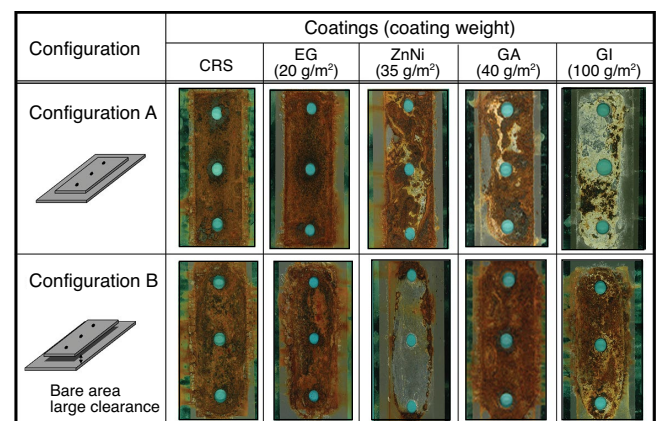


FIGURE 5. Appearance of disassembled specimens (large piece) of Configurations A and B at 60 cycles.

Figure 6 shows a comparison of the influence of coating weight on perforation corrosion between Configurations A and B. Open symbols represent the data for Configuration A and solid symbols represent the results from Configuration B. Regression lines and curves representing the coating weight dependence of the corrosion depth on pure zinc coatings, such as EG and GI, are also shown in this figure. With the pure zinc coatings, perforation corrosion resistance tended to improve as the coating weight increased with both Configurations A and B. However, the corrosion depth of the pure zinc coating with Configuration B was deeper than with Configuration A. A larger crevice gap and bare area in the crevice tended to accelerate perforation corrosion of the pure zinc coatings, including EG and GI. The corrosion behaviors of the zinc alloy coatings, such as GA and ZnNi, were different from those of the pure zinc coatings. In the case of Configuration B, the corrosion resistance of the ZnNi alloy coating was remarkably better than those of EG and GI. In particular, from the regression line, the corrosion depth of ZnNi-coated steel is expected to be one-third that of a pure zinc coating with the same coating weight. This appears to imply that the type of coating is the dominant factor for improving perforation corrosion resistance. On the other hand, no remarkable difference was observed with regard to corrosion between the pure zinc and ZnNi alloy coatings when the specimen type was configuration A. This can be seen by the fact that the corrosion depths of ZnNi and GA essentially coincided with the regression curve drawn from the data for the pure zinc coatings. This would suggest that the coating weight is the dominant factor for corrosion resistance, regardless of the type of coating.

Electrodeposition Throwing Power

A bare area was formed when a lapped specimen with a large crevice gap was painted with plastic spacers in the crevice because the spacers prevented the liquid paint from entering the crevice. However, objects, such as plastic spacers, do not normally appear in the crevice in actual automotive parts. Therefore, in actual manufacturing processes, even the inside of the lapped portions can be painted, depending on the crevice gap. The appearances of disassembled GI 100 g/m² specimens painted without the spacers after 30 cycles are shown in Figure 7. A larger crevice gap enables easy entry of phosphating and paint solutions into the lapped portion. As a result, the throwing power of the paint in the crevice increased as the gap increased. The extent of corrosion damage became smaller with an increasing crevice gap. When the crevice gap was 300 μm, the inside of the crevice was completely covered with paint, and corrosion was substantially prevented. It is believed that the true gap of the crevice in the lapped specimen is almost the same when the specimens were painted without the spac-

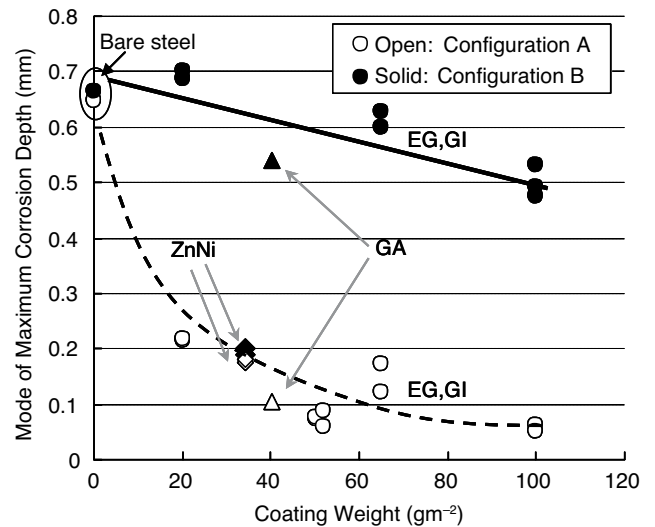


FIGURE 6. Effect of coating weight on corrosion depth on Configurations A and B at 60 cycles.

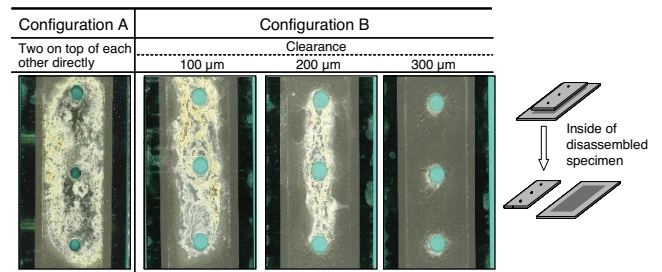


FIGURE 7. Appearance of disassembled GI 100 g/m² specimens (large piece) prepared without the spacers at 30 cycles.

ers. Paint throwing power controls the crevice gap so that paint can no longer enter inside the crevice. From this, it is estimated that there were no large variations in corrosion damage because the true crevice gap was almost constant.

Accumulation and Outflow of Corrosion Product in the Crevice

The corrosion loss of the GI coating and the amount of corrosion product after 60 cycles quantified by ICP measurements are shown in Figure 8. The larger crevice gap led to higher corrosion rates and increased corrosion loss. The corrosion rate in the intentional 300 μm gap was 1.6 times greater than in the gap without intentional control. Approximately 50 g/m² of zinc remained as a corrosion product in the crevice when the gap was less than 200 μm. However, the remaining zinc was less than 40 g/m² when the gap was 300 μm. Because corrosion loss can be regarded as equivalent to the total amount of corrosion product formed during a corrosion test, the difference between the two curves corresponds to the corrosion product that flowed out from the lapped portion. The retention rate of the corrosion product

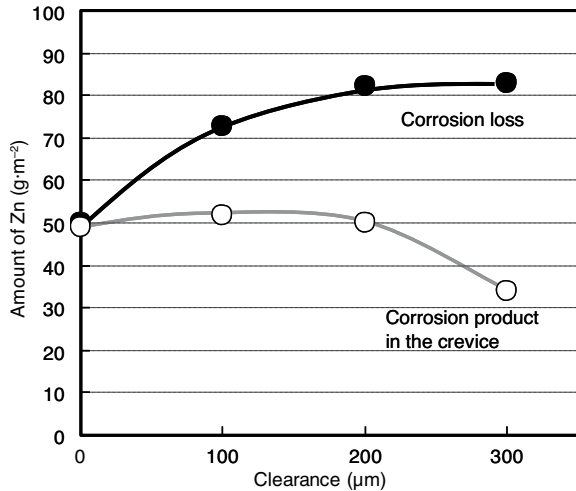


FIGURE 8. Corrosion loss and amount of corrosion product in the crevice as a function of clearance of lapped specimen at 60 cycles.

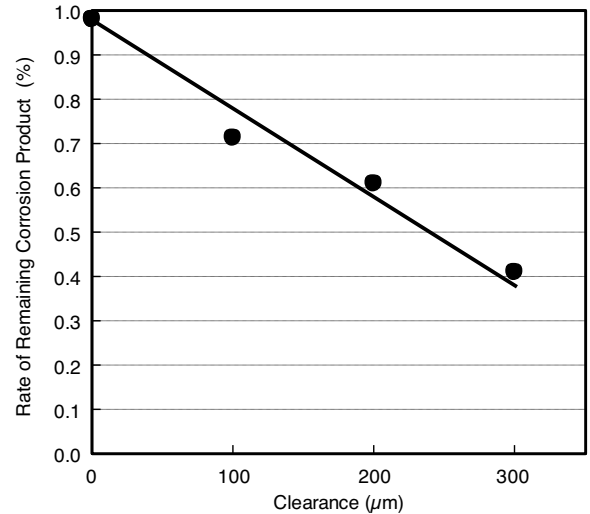


FIGURE 9. Rate of remaining corrosion product in the crevice as a function of clearance at 60 cycles.

as a function of the crevice gap is shown in Figure 9. Almost all the corroded zinc accumulated in the crevice as a corrosion product when the crevice gap of the lapped portion was not intentionally controlled. However, as the crevice gap increased, the remaining zinc corrosion product decreased, and when the crevice gap was 300 μm, less than half of the total amount of corrosion product remained in the crevice. It is believed that a larger crevice gap facilitates corrosion product outflow from the lapped portion concomitant with its acceleration of corrosion of the coating.

Polarization Behavior of Zinc-Coated Steels

The polarization curves of GI, GA, and ZnNi measured in a 5 wt% NaCl solution in air are shown in Figure 10. Because the two curves measured under the same test conditions were similar, a graph was drawn using representative data. The corrosion potential of GI (the pure zinc coating) was the least noble, and a diffusion-limited current density resulting from oxygen diffusion limitation was seen in the cathodic curve. The corrosion potential of GA was noble compared to that of GI because the coating contains iron, which has a more noble corrosion potential than zinc. ZnNi had the noblest potential among the coatings and its cathodic current of the oxygen reduction reaction near the corrosion potential was an order of magnitude lower than those of the others.

Figure 11 shows the polarization curves measured in a deaerated 5 wt% NaCl solution. The polarization curves of all the coatings shifted to less noble potentials compared with those measured in air. The tendency of the corrosion potential dependence on the coating type was the same as that observed in air. The above-mentioned, diffusion-limited current density by oxygen diffusion limitation in the cathodic curves was not observed in this case because the concentration of oxygen in the solution was very low. For this reason,

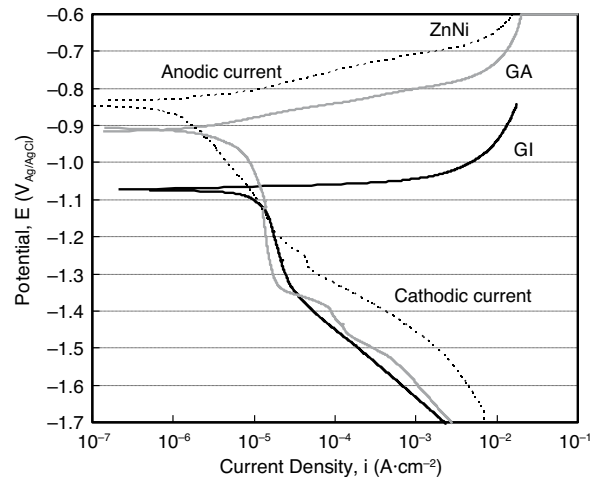


FIGURE 10. Polarization curves of coated steel sheets in 5 wt% NaCl solution under atmospheric conditions.

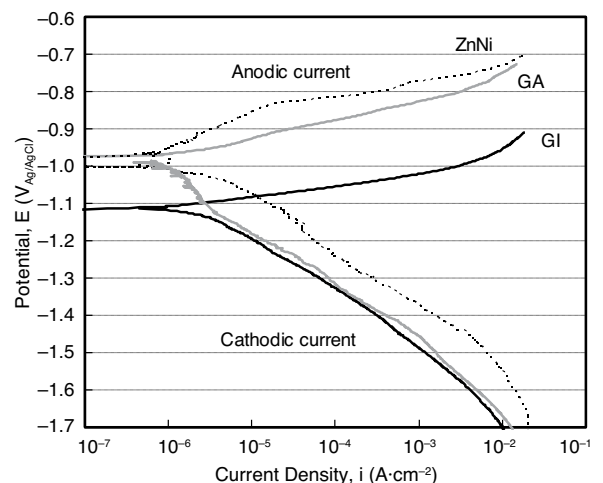


FIGURE 11. Polarization curves of coated steel sheets in deaerated 5 wt% NaCl solution.

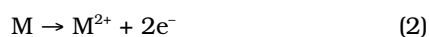
the cathodic current near the corrosion potential was almost the same, regardless of the type of coating.

DISCUSSION

Influence of Specimen Configuration on Corrosion Behavior of Coatings

Different configurations of lapped specimens yielded different results in the corrosion test. In particular, an intentionally controlled bare area in the crevice and the crevice gap of the lapped portion had a significant influence on corrosion resistance. The corrosion resistance of zinc alloy coatings, particularly ZnNi, was superior to that of the pure zinc coatings when a bare area existed in a large gap. On the other hand, the corrosion resistance of pure zinc coatings, such as EG and GI, significantly deteriorated in the specimens with a bare area and a large gap compared to the specimens without intentional control of the bare area and crevice gap. Considering the real automobile manufacturing process, the metal surface inside the crevice should be painted when the lapped portion has a sufficiently large gap, as shown in Figure 7. Therefore, it is believed that a situation in which a larger crevice exists simultaneously with a bare (unpainted) area is incompatible with the real situation. In addition, there have been reports that coating weight is the dominant factor for perforation corrosion in vehicles in service. Rendahl investigated perforation corrosion in the lapped portion of vehicles used in Northern Europe and reported that perforation corrosion was suppressed as the coating thickness increased.²³ Fujita and Mizuno clarified the fact that the main controlling factor affecting perforation corrosion was the coating weight regardless of the type of coating, even in corrosion tests, provided that the corrosion behavior in the test had a good correlation with that in vehicles in service.²⁴ In terms of the structure of the lapped portion and the corrosion-controlling factor in real situations, it is believed that Configuration A, i.e., no intentional bare area in the crevice and a small gap, can reproduce the corrosion behavior in actual vehicle environments.

A larger crevice gap of the lapped specimen allows more corrosive solution and oxygen to be supplied in the crevice. The anodic reaction of zinc-coated steel in a neutral pH solution is the metal dissolution process expressed by Equation (2). The cathodic reaction is the oxygen reduction reaction in Equation (3):



In the case of GI and GA, a limited current was observed since the rate-determining step of the oxygen reduction reaction is the diffusion of oxygen from the bulk solution to the metal surface (through a dif-

fusion layer), as shown in Figure 10. The diffusion-limited current density, i_{Lim} , as a result of the oxygen diffusion limitation, is expressed in Equation (4):

$$i_{Lim} = \frac{zFD_{O_2}C_{O_2}}{\delta} \quad (4)$$

where z is the charge number, F is Faraday's constant, D_{O_2} is the diffusion coefficient of oxygen in the solution, and C_{O_2} is the concentration of oxygen in the bulk solution. On the other hand, although a sufficient amount of oxygen exists near the surface, a limiting current was not observed in the cathodic curve of the ZnNi coating. The corrosion rate of ZnNi seemed to be an order of magnitude lower than those of the other coatings in the bulk solution. In addition, potential dependence on the cathodic current was observed at -1.0 V to -0.9 V in the cathodic curve of the ZnNi coating in Figure 10. The rate of the cathodic reaction due to oxygen reduction was controlled by both the reaction and by diffusion, and resulted in a lower corrosion rate. The addition of nickel to zinc coatings is considered to suppress the oxygen reduction reaction. It is also possible that the corrosion product of the ZnNi coating gives a different electrochemical property from those of other coatings. When the crevice gap is large, as in Configuration B, the solution in the crevice can be regarded as bulk solution since a large volume of solution and air can enter. The corrosion behavior in those environments is believed to be attributable to the electrochemical properties, similar to the polarization curves in bulk solution in air. Therefore, the corrosion rate of the pure zinc coatings was higher than that of ZnNi because of the difference in the oxygen reduction reactions, and consequently, the pure zinc coating dissolved in a shorter time.

On the other hand, in the deaerated solution, no remarkable difference in the cathodic current was observed near the corrosion potential among the three coatings, as shown in Figure 11. When the crevice gap of a lapped specimen is very small, as in configuration A, solution properties, such as the concentration of ions and the pH, can change easily. As a result, corrosion product efficiently forms and accumulates in the crevice. The amount of oxygen contained in the solution in the crevice can be low, since convection of the solution does not occur in the crevice filled with corrosion product. Therefore, it is believed that the coating weight is a dominant factor and no remarkable differences in perforation corrosion resistance were observed between the pure zinc coatings and the zinc alloy coatings with the same coating weight, as shown in Figure 6.

The corrosion product is believed to be another significant factor in determining perforation corrosion in the crevice. Fujita proposed that perforation corrosion can be divided into four periods: (i) corrosion of the zinc coating itself, (ii) sacrificial corrosion of

the zinc coating coupled with the steel substrate, (riii) inhibition of corrosion of the steel substrate by the zinc corrosion product, and (riv) corrosion of the steel substrate until perforation.²⁵ In the case of pure zinc, the period τ_i , during which the zinc coating itself is corroded, will be shortened if a sufficient amount of oxygen to accelerate the cathodic reaction is supplied in the crevice, as discussed above. In addition, a large amount of salt water and humid air introduced by the large crevice gap can facilitate dissolution and outflow of the corrosion product from the lapped portion. Therefore, the corrosion inhibition effect of the corrosion product cannot be expected when the specimens have a large crevice gap and a shortened duration of τ_{iii} results. Zhu, et al., measured impedance in the lapped portion and discussed the influence of oxygen supply in the crevice on the corrosion rate.²⁶ Their research indicated that the corrosion rate was highest when the crevice gap was 250 μm ; the corrosion rate in that study shows good agreement with the results of the present study.

Optimum Test Specimen for Perforation Corrosion Evaluations

As discussed in earlier sections, as long as conventional coatings are evaluated, the main controlling factor affecting perforation corrosion in vehicles in service is the coating weight. In terms of the influence of coating weight on perforation corrosion, it is believed that configuration A, which had no large crevice gap and no intentional bare area in the crevice, can reproduce the electrochemical properties and physical effects of the corrosion products in the crevice that can be expected to occur in real automotive parts. In addition, assuming the crevice gap is large, the inside of the crevice of the lapped portion would be painted in the actual automotive manufacturing process, and this paint coating can serve to prevent severe corrosion. Therefore, specimens with a bare area in a large crevice are not believed to reproduce the environments of lapped portions in real vehicles. Because the corrosion mechanism is different, use of this type of specimen can degrade the inherent corrosion resistance of the zinc coating, and so can give misleading results for the development and selection of materials.

The portions where perforation corrosion occurs in vehicles in service are lapped portions where steels are in direct, mutual contact and are welded or mechanically jointed. The bare area and the true clearance are formed naturally, not intentionally, by phosphating and electrodeposition after assembly. On the basis of this study, it can be proposed that the specimens for evaluating perforation corrosion resistance should be prepared in accordance with the actual manufacturing process, without intentional adjustments, to result in the reproduction of corrosive environments and corrosion behaviors at lapped portions in real automobiles.

CONCLUSIONS

The influence of the test specimen configuration on the corrosion behavior of zinc-coated steel sheets in accelerated corrosion tests was investigated. An appropriate specimen configuration for perforation corrosion testing was proposed on the basis of a comparison with the corrosion behavior observed in vehicles in service. The major findings of this study are as follows:

- ❖ The controlling factor for perforation corrosion resistance depends on the configuration of the test specimen. The apparent corrosion resistance of zinc alloy coatings is superior to those of pure zinc coatings if the specimen has an intentional bare area in a large crevice of the lapped portion.
- ❖ The coating weight is the main factor controlling perforation corrosion when the specimen is assembled by jointing steel sheets in direct mutual contact in a manner similar to the real structure of automobiles.
- ❖ A bare area in the crevice and a large crevice of the lapped portion accelerate corrosion of pure zinc coatings in comparison with zinc alloy coatings as a result of the rapid consumption of the coating and outflow of the corrosion product in the crevice.
- ❖ It is proposed that specimens for evaluating perforation corrosion resistance should be prepared in accordance with the actual automotive manufacturing process without creating an intentional bare portion and large crevice gap.

REFERENCES

1. F.O. Wood, "Deicing Salt Usage in North America," CORROSION/78, paper no. 7 (Houston, TX: NACE International, 1978).
2. Y. Nagata, T. Hamanaka, "Status and Prospect of Japanese Automotive Anticorrosion Technology," Proc. 5th Automotive Corrosion and Prevention Conf., paper no. P-250 (Warrendale, PA: SAE, 1991), p. 7-15.
3. T. Hada, "Present and Future Trends of Coated Steel Sheet for Automotive Use," Proc. Int. Conf. on Zinc and Zinc Alloy-Coated Steel Sheet (GALVATECH 89) (Tokyo, Japan: ISIJ, 1989), p. 111-119.
4. S. Sugimoto, "Expectation for Automotive Coated Steel Sheet in View of Cost and Global Supplyability Needs," Proc. Int. Conf. on Zinc and Zinc Alloy-Coated Steel Sheet (GALVATECH 98) (Tokyo, Japan: ISIJ, 1998), p. 64-69.
5. M.L. Stephens, "SAE ACAP Division 3 Project: Evaluation of Corrosion Test Methods," Proc. Automotive Corrosion and Prevention Conf., P-228, paper no. 892571 (Warrendale, PA: SAE, 1989), p. 157-164.
6. R. Boboian, "Advances in Automotive Corrosion Resistance," Proc. 13th Int. Corros. Cong., paper no. 076 (Melbourn, Australia: Australasian Corrosion Association, 1996), p. 378-386.
7. Summary of Corrosion Testing of Automotive Materials International Seminar (Stockholm: Swedish Corrosion Institute, 2000).
8. N. LeBozec, D. Blandin, D. Thierry, *Mater. Corros.* 59, 11 (2008): p. 889-894.
9. SAE International Surface Vehicle Standard, SAE J2334 "Cosmetic Corrosion Lab Test" (Warrendale, PA: SAE, 1998).
10. H.E. Townsend, "Status of a Cooperative Effort by the Automotive and Steel Industries to Develop a Standard Accelerated Corrosion Test," Proc. Automotive Corrosion and Prevention Conference P-228, paper no. 892569 (Warrendale, PA: SAE, 1989), p. 133-145.
11. L.A. Roudabush, "Update on the Development of an Improved Cosmetic Corrosion Test by the Automotive and Steel Industries,"

- H.E. Townsend, D.C. McCune, Proc. 6th Automotive Corrosion and Prevention Conf. P-268, paper no. 932334 (Warrendale, PA: SAE, 1993), p. 53-83.
12. H.E. Townsend, M.W. Simpson, W.B. van der Linde, D.C. McCune, *Corrosion* 55, 4 (1999): p. 406-411.
13. D. Davidson, L. Thompson, F. Lutze, B. Tiburcio, K. Smith, C. Meade, T. Mackie, D. McCune, H. Townsend, R. Tuszynski, Special Publication SP-1770, H0575B (Detroit, MI: Society of Automotive Engineers, 2003), p. 45-63.
14. S. Fujita, D. Mizuno, *Corros. Sci.* 49 (2007): p. 211-219.
15. N. Shibata, H. Kunimi, *Trans. ISIJ* 28 (1988), p. 578.
16. Y. Ito, Y. Miyoshi, "Corrosion Protection of Galvanized Steel Sheet-Corrosion Investigation of Field Vehicle and Its Laboratory Evaluation Methods," Proc. Automotive Corrosion and Prevention Conf. Expo. P-228, paper no. 892580 (Warrendale, PA: SAE, 1989), p. 217-227.
17. R. Brady, A. Yahkind, A. Kowalski, L. Price, "Effects of Cyclic Test Variables on the Corrosion Resistance of Automotive Sheet Steels," Proc. Automotive Corrosion and Prevention Conf. Expo. P-228, paper no. 892567 (Warrendale, PA: SAE, 1989), p. 121-126.
18. M. Nakazawa, Y. Miyoshi, D. Davidson, "Corrosion Investigation from 10-Year Field Exposure Vehicles," CORROSION/95, paper no. 375 (Houston, TX: NACE, 1995).
19. M. Strom, G. Strom, G. Strannhage, "Making the Best of Corrosion Testing," Proc. Eurocorr 2006 Maastricht (Maastricht, The Netherlands: Nederlands Corrosie Centrum, 2006), p. 25-28.
20. International Standard ISO 8407:1991(E), "Corrosion of Metals and Alloys-Removal of Corrosion Products from Corrosion Test Specimens" (Geneva, Switzerland: ISO, 1991).
21. T. Shibata, *Corrosion* 52 (1996): p. 813-830.
22. S. Fujita, H. Kajiyama, C. Kato, *JFE Technical Report* 4 (2004), p. 9-16.
23. B. Rendahl, "Evaluation of Corrosion Protection on Recent Model Vehicles," CORROSION/98, paper no. 741 (Houston, TX: NACE, 1998).
24. S. Fujita, D. Mizuno, *Corros. Sci.* 49 (2007): p. 211-219.
25. S. Fujita, "Perforation Corrosion and Its Mechanism of Galvanized Steel Sheets on Vehicles," CORROSION/98, paper no. 541 (Houston, TX: NACE, 1998).
26. F. Zhu, S. Hedlund, D. Thierry, *Br. Corros. J.* 31, 2 (1996): p. 113-118.
-